Full paper/Mémoire

Silica/A153–SO₃H: An efficient catalyst for the Baeyer–Villiger oxidation of cyclic ketones with hydrogen peroxide

Wanzhen Xing, Qingguo Ma, Xinhua Peng *

School of Chemical Engineering, Nanjing University of Science and Technology, Nanjing 210094, China

A B S T R A C T

Silica/A153–SO₃H was prepared and characterized by FT–IR, TG and SEM. It proved to be an efficient and recyclable heterogeneous catalyst in the Baeyer–Villiger (BV) oxidation of cyclic ketones with H_2O_2 as an oxidant. Catalysts with different silica particle sizes were also made comparisons in terms of catalytic effect.

© 2014 Académie des sciences. Published by Elsevier Masson SAS. All rights reserved.

1. Introduction

Baeyer–Villiger (BV) oxidation is one of the most important organic chemical reactions with a large range of possible applications, including synthesis of the agrochemical, chemical and pharmaceutical industries [1–3]. The oxidants used in the traditional Baeyer–Villiger oxidation are organic peracids [4] and potassium mono-peroxysulfate [5], which potentially produce large amounts of harmful and expensive-to-handle wastes. Green oxidants, such as hydrogen peroxide [6,7], alkyl hydroperoxides [8] and molecular oxygen [9] were widely used in recent years. Hydrogen peroxide is a more promising oxidant for BV reaction, with a number of advantages: it is a cheap, environmentally benign reagent with high content of active oxygen, and water is formed as the only by-product. Due to the ease of separation and the prospect of easily recycling the catalyst for subsequent catalytic reactions, several heterogeneous catalytic systems have been reported, such as polymeranchored metal complexes [10], solid acid [11], Sn-MCM-41 [12], sulphonated resins [13], titanium silicalites [14], transition metal-functionalized hydrotalcites [15], hydrotalcite-supported Sn catalyst [16], Sn-synthesized hydrotalcites [17], and supported-MTO catalyst [18]. To suffer from some disadvantages like low activity or selectivity, cost, and the need for high concentrations of H_2O_2, there is still an increased demand for heterogeneous catalytic systems.

Silica nanoparticles have been used in a myriad of diverse applications, such as catalysis, humidity sensors, electronic, drug delivery, pigments [19–21]. With the silanol groups in the silica structure, several studies have been published on reactions of silica surface silanol groups with organic compounds [22,23]. H^+ can catalyze the reaction according to the mechanism of the BV reaction [24], therefore sulfonic acid group (–SO₃H) was introduced into silica through phenyltrimethoxysilane (A153) in our experiments. The results showed that the prepared catalyst was efficient and recyclable for BV oxidation with H_2O_2.

* Corresponding author.
  E-mail address: xhpeng@mail.njust.edu.cn (X. Peng).
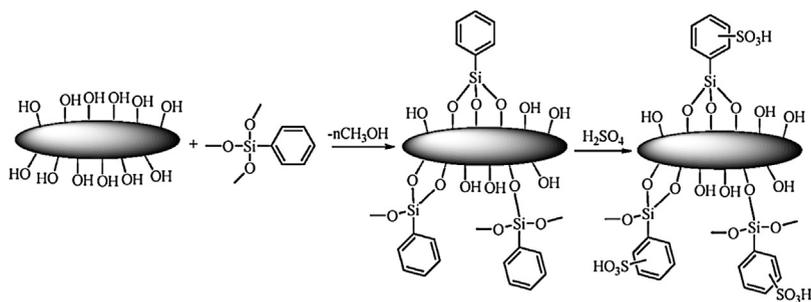
Scheme 1. Preparation of the catalyst.

2. Experimental

2.1. Materials and procedures

Phenyltrimethoxysilane A153 was purchased from Nanjing Chengong Company, silica nanoparticles (20 nm) and silica (200~300 mesh) were obtained from Nanjing Tianxing Company; all cyclic ketones were purchased from Aladdin.

FT–IR spectra were recorded on a Bruker Tensor 27 Fourier-transform infrared spectrometer using KBr tableting technique. The thermal behavior of the sample was studied with Mettler Toledo, TG/SDTA851^e instrument under nitrogen atmosphere (50 mL/min). The sample was heated at a rate of 10 °C/min from 50 °C to 800 °C. The morphology of the obtained catalyst was determined through scanning electron microscopy (SEM) using a JEOL JSM-6380LV made in Japan. A gas chromatographer (Shimadzu GC-2014C) was used to determine the product's composition.

2.2. Preparation of the catalyst

Concentrated hydrochloric acid (10 mL) and silica nanoparticles (2.0 g, 20 nm) were mixed in a flask (20.0 mL), were stirred for 12 h at 80 °C to remove impurities and active hydrophilic group on the silica's surface. The mixture was poured into a large amount of water, then centrifuged and dried at 110 °C for 12 h. A153 (1.0 mL) and ethanol (5.0 mL) were added into flask, acetic acid was added under strong stirring to make A153 hydrolyze. After continuously stirring for 0.5 h, the treated SiO$_2$ nanoparticles powder (1.0 g) was added into the liquid, stirred for 12 h at 80 °C. After the reaction, SiO$_2$/A153 was obtained by centrifugation and dried at 120 °C for 12 h. SiO$_2$/A153 (1.0 g) and ethanol (5.0 mL) were placed into a flask, concentrated sulfuric acid (5.0 mL) was introduced dropwise at room temperature. After stirring for 48 h, the mixture was poured into water (20.0 mL), silica/A153-SO$_3$H was obtained by centrifugation and dried at 120 °C for 48 h. This catalyst was named catalyst A.

In the same way, –SO$_3$H was introduced into silica (200~300 mesh) through A153, the catalyst was named catalyst B.

A blank catalyst was prepared: SiO$_2$ nanoparticles (1.0 g) were placed into a flask, concentrated sulfuric acid (5.0 mL) was introduced dropwise at room temperature.

After stirring for 48 h, the mixture was poured into water (20 mL), the catalyst was obtained by centrifugation and dried at 120 °C for 48 h; this catalyst was named silica–SO$_3$H (Scheme 1).

2.3. Baeyer–Villiger oxidation of cyclic ketones

A typical procedure for the Baeyer–Villiger oxidation was as following: cyclic ketones (2.5 mmol) and 30% hydrogen peroxide (2.5 equiv.) were dissolved in acetonitrile (3.0 mL). After the catalyst (5–20 mg) was added, the mixture was heated to 10–65 °C and stirred for 5–20 h. A saturated solution of NaHCO$_3$ (3 × 3 mL) was added to the reaction mixture and the aqueous phase was extracted with ethyl acetate (3 × 10 mL). The combined organic extracts were dried over MgSO$_4$ and concentrated under reduced pressure. The products in the resulting mixture were determined by GC analysis based on the internal standard (nonane).

3. Results and discussion

3.1. FT–IR spectra of the catalyst

Fourier-transform infrared (FT–IR) spectra analysis of silica nanoparticles, silica/A153 and silica/A153–SO$_3$H (catalyst A was the same as catalyst B) were reported in Fig. 1. A very strong absorption band at about 1100 cm^{-1}
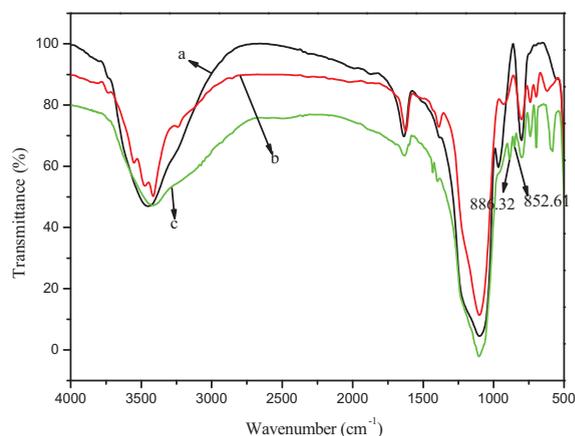

Fig. 1. (Color online.) FT–IR spectra for (a) silica (b) silica/A153 (c) silica/A153-SO$_3$H.
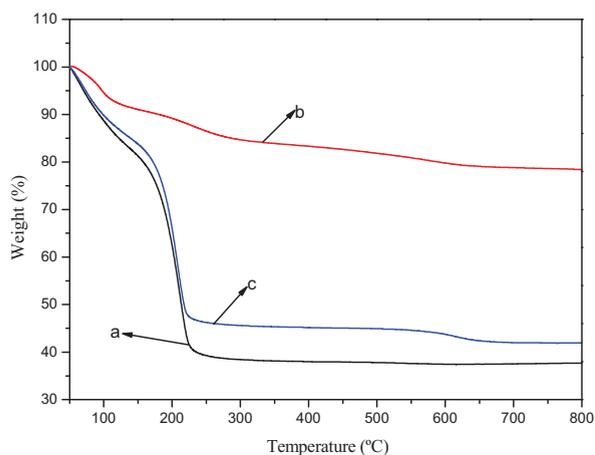
Fig. 2. (Color online.) TGA for (a) catalyst A, (b) catalyst B, (c) 5-fold-reused catalyst A.

was attributed to the stretching vibrations of Si–O–Si groups, while the bending modes of these groups corresponded to the band observed at about 470 cm^{-1}. The band at 802 cm^{-1} was assigned to Si–O stretching vibration. The peak at 3420 cm^{-1} was associated with the stretching vibrations of Si–OH groups. In the spectra of silica/A153, the absorptions at 700 cm^{-1} was C–Si group. A band at 3415 cm^{-1} was observed as a result of asymmetric stretching vibrations of the methyl groups. A band at 1432 cm^{-1} was attributed to the vibration of the phenyl group. S–O stretching mode was observed at nearly 886 and 852 cm^{-1}. These signals suggested the existence of A153 and–SO_3H in the silica structure.

3.2. The TGA and SEM of the catalysts

TG analysis was applied to characterize the thermal stability and capacity of the prepared catalyst. Fig. 2 displays the TGA curves of catalyst A, catalyst B and 5-fold-reused catalyst A samples. For catalyst A, the weight loss of

about 14% at 120 °C was related to physically combined water, the weight loss of about 50% between 120 °C and 550 °C was attributed to the organics on the silica nanoparticles, the third weight loss was about 2% at 550–750 °C, indicating chemically the dehydroxylation of combined water and silanol groups on silica nanoparticles, while for catalyst B, the organic weight loss at 120~600 °C was only of about 13%. Owing to larger specific surface and more amount of silicon hydroxyl on silica nanoparticles, more capacity was on catalyst A. As shown in Fig. 3, the analysis of the SEM images showed that the morphology of silica nanoparticles was irregular and gathered due to the small size of the silica particles, the surface of catalyst A becoming denser when compared with pure silica (Fig. 3a and b). The surface of silica was relatively smooth while the surface of the catalyst B was slightly rough (Fig. 3c and d), which could evidence the fact that organics were more easily introduced into the surface of the silica nanoparticles. This result was in agreement with TG results. From the TG analysis of 5-fold reused catalyst A samples, the capacity was reduced by about 8% compared with the new one, which proved the reproducibility of the catalyst. As could be seen from Fig. 3e, the morphology of catalyst A did not change obviously after reusing it 5 times. TG analysis also suggested that the catalyst was suitable for the temperature of BV oxidation.

3.3. The acidity of catalyst A and catalyst B

Catalyst A (1.0 g) was soaked in an NaOH solution (50 mL, 0.1 $mol \cdot L^{-1}$) for 24 h, 2 drops of methyl orange TS were added into the supernatant (10 mL); chemical titration was carried out by dropwise addition of a 0.1 $mol \cdot L^{-1}$ HCl solution; the acidity of catalyst A was estimated on the consumption of the NaOH solution. The evaluated acidity was 2.34 $mmol \cdot g^{-1}$, whereas that of catalyst B was 0.81 $mmol \cdot g^{-1}$. Acidity was calculated using the formula given in Equation (1):

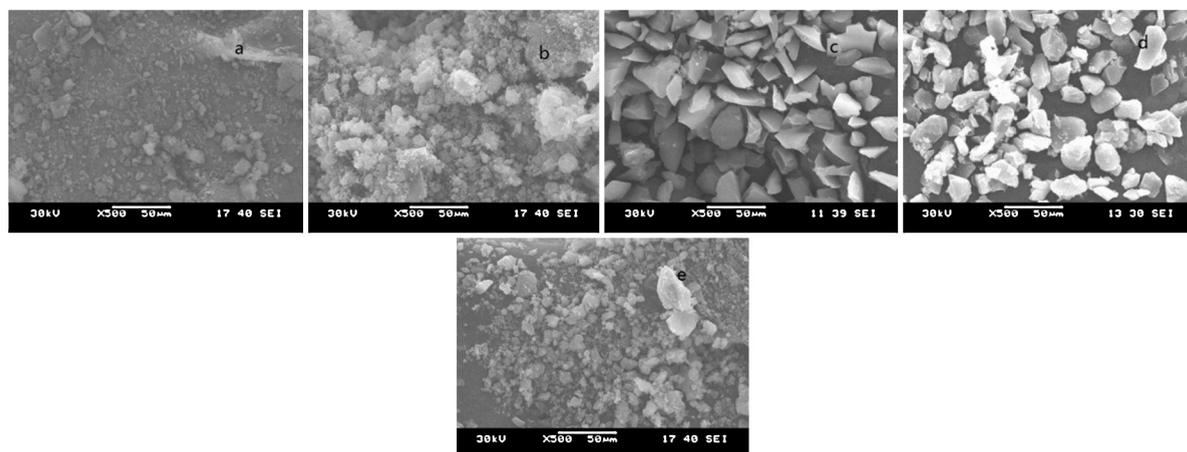$$H = (10-V) \times 0.1 \times 5/m \qquad (1)$$

Fig. 3. SEM images for (a) silica (20 nm), (b) catalyst A, (c) silica (200–300 m), (d) catalyst B, (e) 5-fold-reused catalyst A.

Table 1
Oxidation of 2-adamantanone with different catalysts[a].

Entry	Catalyst	Conversion (%)[b]	Yield (%)[b]
1[c]	Silica	9	5
2[c]	Silica–A153	8	5
3	Silica–SO$_3$H	9	6
4[d]	A153–SO$_3$H	99	95
5	Catalyst A	99	96
6	Catalyst B	49	45

[a] 2-Adamantanone: 2.5 mmol; 30% aq. H$_2$O$_2$: 1.5 mL, 2.5 equiv.; acetonitrile: 3.0 mL; time: 15 h; catalyst: 10 mg; temperature: 45 °C.
[b] Conversion and yield were determined by GC analysis based on the internal standard (nonane).
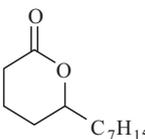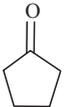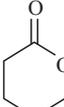[c] Silica nanoparticles.
[d] A153-SO$_3$H (2.0 mL).
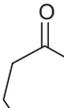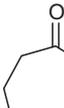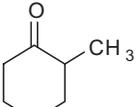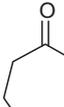
where H is the acidity of the catalyst (mmol·g^{-1}), V is the amount of NaOH used for titration (mL), m is the amount of catalyst A used in titration (g).

3.4. Application of catalysts in the Baeyer–Villiger reaction

The comparison of the results obtained with different catalysts using 2-andamantanone as a substrate was

Table 2
Reusability of catalyst A on the example of 2-andamantanone oxidation[a].

Entry	Conversion (%)[b]	Yield (%)[b]	Catalyst recovered (%)
1	99	96	95
2	95	91	93
3	92	90	91
4	88	85	90
5	85	81	90

[a] Reaction conditions: 2-andamantanone, 2.5 mmol; catalyst A, 10 mg; 30% aq. H$_2$O$_2$, 1.5 mL, 2.5 equiv.; acetonitrile, 3.0 mL; temperature, 45 °C.
[b] Conversion and yield were determined by GC analysis based on the internal standard (nonane).

reported in Table 1. As can be seen in Table 1, 2-andamantanone was not oxidized by silica, silica/A153 and silica–SO$_3$H are in their optimum reaction conditions. Although the catalytic effect was significant, A153–SO$_3$H was not considerable due to its unrepeatability as a homogeneous catalyst. The sulfonic acid group could not be introduced directly to silica nanoparticles under the same conditions (whose FT–IR spectrum was the same as that of silica nanoparticles), so the catalytic effect was weak. In a word, catalyst A was selected as the best catalyst

Table 3
Baeyer–Villiger oxidation of the ketones catalyzed by catalyst A[a].

Entry	Substrate	Temperature (°C)	Time (h)	Conversion (%)[b]	Yield (%)[b]	Product
1		45	20	98	95	
2		10	20	53	45	
3		65	5	61	55	
4		45	15	99	96	
5		65	20	15	8	
6		45	20	97	93	
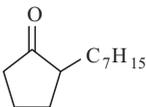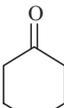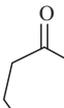
[a] Reaction conditions: substrate, 2.5 mmol; 30% aq. H$_2$O$_2$, 1.5 mL, 2.5 equiv; acetonitrile, 3.0 mL; catalyst A, 10 mg.
[b] Conversion and yield were determined by GC analysis based on the internal standard (nonane).
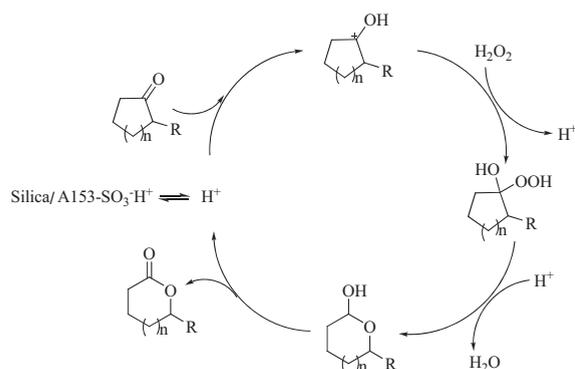
Scheme 2. A possible mechanism for Baeyer–Villiger oxidation over silica/A153-SO$_3$H [24].

for reactions in terms of catalytic effect and reusability in this article. Catalyst A appeared to be much more active than catalyst B due to the fact that it contains more –SO$_3$H groups (entry 6).

$$\text{Conversion}(\%) = \frac{\text{moles of reactant consumed}}{\text{initials moles of the reactant}} \times 100 \quad (2)$$

$$\text{Yield}(\%) = \frac{\text{moles of corresponding lactone}}{\text{initials moles of the reactant}} \times 100 \quad (3)$$

After completion of the reaction, the catalyst was recovered by centrifugation and dried at 120 °C; reusability studies were performed for 2-andamantanone oxidation under the same reaction conditions for five runs; the results showed a very high but slowly declining catalyst activity (Table 2).

Finally, Table 3 summarizes the reaction of simple cyclic ketones in the presence of catalyst A; cyclic ketones were oxidized to their corresponding lactones under mild conditions within reasonable reaction times. The most reactive of these cyclic ketones studied in this article appeared to be 2-andamantanone, because its ring strain was very high [25]. Non-strained cycloheptanone was much more difficult to oxidize. The low selectivities of cyclopentanone and cyclohexanone were due to the formation of δ-valerolactone and δ-caprolactone in the first step, which subsequently hydrolyzed to their corresponding hydroxyacid. Owing to the fact that the alkyl group bonded to the carbonyl carbon was secondary alkyl, the conversion and yield of 2-heptylcyclopentanone and 2-methylcyclohexanone were high.
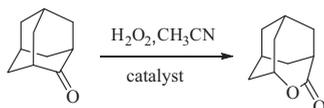
4. Conclusions

The prepared catalyst silica/A153–SO$_3$H showed most important advantages: high activity, good stability, and reusability demonstrated in the Baeyer–Villiger oxidation of various cyclic ketones to the corresponding lactones under mild conditions. FT–IR, TG and SEM confirmed the structure, capacity and morphology, and the acidity of catalyst A was also determined. The catalyst with silica nanoparticles showed better catalytic activity. The preparation process is nontoxic and cheap, and is environment friendly (Scheme 2).

References

[1] R. Bernini, A. Coratti, G. Fabrizi, A. Goggiamani, Tetrahedron Lett. 44 (2003) 8991–8994.
[2] M. Renz, B. Meunier, Eur. J. Org. Chem. 1999 (1999) 737–750.
[3] G. Brink, I. Arends, R. Sheldon, Chem. Rev. 104 (2004) 4105–4123.
[4] P. Park, A.P. Kozikowski, Tetrahedron Lett. 29 (1988) 6703–6706.
[5] A. Chrobok, Tetrahedron 66 (2010) 6212–6216.
[6] A. Yoshida, M. Yoshimura, K. Uehara, S. Hikichi, N. Mizuno, Angew. Chem. Int. Ed. 45 (2006) 1956–1960.
[7] S. Baj, A. Chrobok, Synth. Commun. 38 (2008) 2385–2391.
[8] B. Dutta, S. Sreyashi Jana, H. Bhunia, S. Honda, Koner, Appl. Catal., A 382 (2010) 90–98.
[9] Y.F. Li, M.Q. Guo, S.F. Yin, L. Chen, Y.B. Zhou, R.H. Qiu, C.T. Au, Carbon 55 (2013) 269–275.
[10] C. Palazzi, F. Pinna, G. Strukul, J. Mol. Catal. A: Chem. 151 (2000) 245–252.
[11] J. Fischer, W.F. Holderich, Appl. Catal. A: Gen. 180 (1999) 435–443.
[12] A. Corma, M.T. Navarro, M. Renz, J. Catal. 219 (2003) 242–246.
[13] W. Hoelderich, J. Fischer, G. Schindler, P. Arntz, German Patent DE (1999) 19745442.
[14] B. Notari, Adv. Catal. 41 (1996) 253–334.
[15] K. Kaneda, S. Ueno, T. Imanaka, J. Mol. Catal. A: Chem. 102 (1995) 135–138.
[16] Y. Liu, C.L. Chen, N.P. Xu, Chin. J. Catal. 25 (2004) 801–804.
[17] R.P. Unnikrishnan, S.D. Endalkachew, J. Mol. Catal. A: Chem. 191 (2003) 93–100.
[18] R. Bernini, E. Mincione, M. Cortese, R. Saladino, G. Gualandi, M.C. Belfiore, Tetrahedron Lett. 44 (2003) 4823–4825.
[19] A.V. Rao, S.D. Bhagat, H. Hirashima, G.M. Pajonk, J. Colloid Interf. Sci. 300 (2006) 279–285.
[20] J. Ge, Q. Zhang, T. Zhang, Y. Yin, Angew. Chem. Int. Ed. 120 (2008) 9056–9060.
[21] Y. Zhu, J. Shi, W. Shen, X. Dong, J. Feng, M. Ruan, Y. Li, Angew. Chem. Int. Ed. 117 (2005) 5213–5217.
[22] J. Lin, H. Chen, Y. Ji, Y. Zhang, Colloids Surf. A 411 (2012) 111–121.
[23] M.M. Pohl, J. Radnik, M. Schneider, U. Bentrup, D. Linke, A. Brückner, E. Ferguson, J. Catal. 262 (2009) 314–323.
[24] Q. Long, H. Ji, S. Lu, J. Mol. Struct.: Theochem 901 (2009) 117–127.
[25] A. Drozd z, A. Chrobok, S. Baja, K. Szymanska, J. Mrowiec-Białon, A.B. Jarzebski, Appl. Catal. A: Gen. 467 (2013) 163–170.